Although a low-activity energy expenditure and a low number of steps were risk factors for frontal lobe atrophy progression in male participants, they were not risk factors in female participants (Tables 4 and 5). Generally, there are many more men with brain atrophy than women (38). In this study, the ratios of frontal lobe atrophy progression were different between male and female participants (Table 2). Sex hormones may also affect the relationship between physical activity and frontal lobe atrophy. Androgens and estrogens are associated with brain volume (13,24), and the adaptability of the brain to physical activity may be higher in men than that in women.

In contrast to activity energy expenditure, total energy expenditure was associated with frontal lobe atrophy progression in both men and women. Basal metabolism is the maximal occupation ratio in total energy expenditure. The brain metabolic rate is included in the basal metabolism. In women, total energy expenditure including basal metabolism appears to be a better index of the risks for frontal lobe atrophy progression compared with physical activity parameters. However, because some of the odds ratios were exceedingly large in female participants, our logistic regression model may not have precisely estimated the risk of frontal lobe atrophy. There were 55 male participants with frontal lobe atrophy progression (Table 2), but only 35 female participants had frontal lobe atrophy progression (Table 2). These sex differences in the brain atrophy progression rate may have influenced estimation of the odds ratio. In women in particular, further investigations may be needed to determine the association of frontal lobe atrophy progression with total energy expenditure.

Brain atrophy is caused in part by obesity (19), metabolic syndrome, and its components (4,12). A high level of physical activity improves obesity and metabolic syndrome (29). Cross-sectional research suggests that prevention of obesity by physical activity causes the relationship between physical activity and brain volume (19). However, in this study, frontal lobe atrophy progression was associated with the physical activity level in logistic regression models that controlled for BMI. Physical activity or the total energy expenditure may be independent factors for preventing frontal lobe atrophy progression, regardless of obesity.

In this study, the activity energy expenditure, the number of steps, and the total energy expenditure were quantitative data collected by an accelerometer. The objectivity of our study is higher than that of past studies that estimated the physical activity level with a questionnaire (5,19).

A limitation of this study is the noninvasive approach using MRI. We could not elucidate the mechanism of frontal lobe atrophy progression induced by a low level of physical activity or total energy expenditure. In an animal study, the beta amyloid cumulative dose is active mass dependent in mouse brain (22). The death of neurons may be inhibited by physical activity. Some growth factors, such as nerve growth factor or brain-derived neurotrophic factor, contribute to neuronal survival or neurogenesis (31,39). The serum level of nerve growth factors fluctuates with physical exercise (16), and thus, exercise stimulus with physical activity may modify expression of nerve growth factors.

Exercise and physical activity have been reported to change the volume of every region of the brain, including the frontal lobe, the temporal lobe, the parietal lobe, and the hippocampus (3,5,8,19). Interestingly, our results showed associations between brain atrophy progression and physical activity or total energy expenditure only in the frontal lobe, but not in the temporal lobe. We hypothesize that the regional differences in brain atrophy progression were due to differences in the patterns of physical activities (including types, intensities, or frequencies). A previous study suggests that increased blood flow in the brain due to physical exercise promotes neurogenesis (30). Blood flow in the brain varies with exercise type and intensity (20,28). In this study, because the activity energy expenditure, the number of steps, and the total energy expenditure data were collected as the total amount per day with accelerometer sensors, the differences in the patterns of physical activities between participants were not determined. Further investigations that define these details may clearly uncover an association between physical activities and regional differences in brain atrophy progression.

In summary, using the longitudinal design of the NILS-LSA cohort, we evaluated the association between brain atrophy progression and daily physical activity and total energy expenditure in 774 community-living, middle-age, and elderly Japanese people with an 8-yr follow-up duration. Our data confirm that low levels of physical activity and total energy consumption are significant predictors of the risk for brain atrophy, and the effect of atrophy suppression is seen only in the frontal lobe. Promoting participation in physical activities may be beneficial in attenuating age-related frontal lobe atrophy and in preventing dementia.

This work was supported by The Research Funding for Longevity Sciences (23–33) from the National Center for Geriatrics and Gerontology, Japan.

The authors thank all of the participants and the health professionals and researchers from the Department for Development of Preventive Medicine, National Center for Geriatrics and Gerontology, who were involved in the data collection and analyses.

The authors report no conflict of interest.

The results of the present investigation do not constitute endorsement by the American College of Sports Medicine.

REFERENCES

1. Ainsworth BE, Haskell WL, Whitt MC, et al. Compendium of physical activities: an update of activity codes and MET intensities. *Med Sci Sports Exerc.* 2000;32(9 suppl):S498–516.
2. Aoyama T, Asaka M, Kaneko K, et al. Amount and intensity of physical activity in relation to cardiorespiratory fitness in Japanese middle-aged and elderly men. *Jpn J Phys Fit Sports Med.* 2010; 59:191–8.
3. Boyke J, Driemeyer J, Gaser C, Büchel C, May A. Training-induced brain structure changes in the elderly. *J Neurosci.* 2008; 28:7031–5.

Osteoporosis Japan

地域在住中高齢者の膝関節変形と膝伸展筋力との関連

松井康素[1)]　竹村真里枝[1)]　原田　敦[1)]　安藤富士子[2)]
李　成喆[3)]　下方浩史[3)]

はじめに

変形性膝関節症（以下，膝OA）の保存的療法において大腿四頭筋筋力訓練の有効性が確かめられている[1)]。一方，膝関節変形と同筋力との関連を調べた疫学的研究は限られている。そこで，地域在住中高年者対象の大規模コホートにおいて，膝関節変形の有無や程度と膝伸展筋力との関連についての検討を行った。

1　対象と方法

「国立長寿医療研究センター・老化に関する長期縦断疫学研究（NILS-LSA）[2)]」の第5次調査に参加した，50歳以上の1,653名（平均年齢65.4±9.3歳）（男性862名，女性791名），3,299膝を対象とした。膝伸展筋力は，竹井機器工業（新潟市）製の測定装置で，左右別に3回ずつ座位にて膝関節90度屈曲位における等尺性筋力を測定し，最大値を採用した。膝関節変形の程度は，膝関節レントゲン荷重位正面像を左右別々に撮影し，Kellgren-Lawrence（KL）分類をもとに5段階に分類し，II度以上を膝OAありとし，また変形程度により0～I度を正常，II度を軽度変形，III～IV度を重度変形と，3段階に分類した。そしてOAの有無，変形程度により，膝伸展筋力に差があるか否かを，一般線形モデルを用い，年齢，BMIを調整した多重比較（Tukey-Kramer法）にて，左右の膝を合わせ，男女別に検討した。統計解析にはSAS ver9.1.3を用いた。

2　結　　果

年代別の膝関節変形のある割合は図1のごとくで，男女とも，また軽度変形，重度変形例ともに，年代が高くなるほど有意に増加していた（p<0.0001）。膝OAの有無により膝伸展筋力を比較した結果においては，男女とも，膝OAの有無では膝伸展筋力に有意差を認めなかったが，変形の程度を3段階別に分けた場合の同筋力（平均±SE）は，女性では正常例25.4±0.26kg，軽度変形例26.0±0.26kg，重度変形例24.4±0.57kgであり，軽度変形と重度変形例の間に有意差を認めた（p

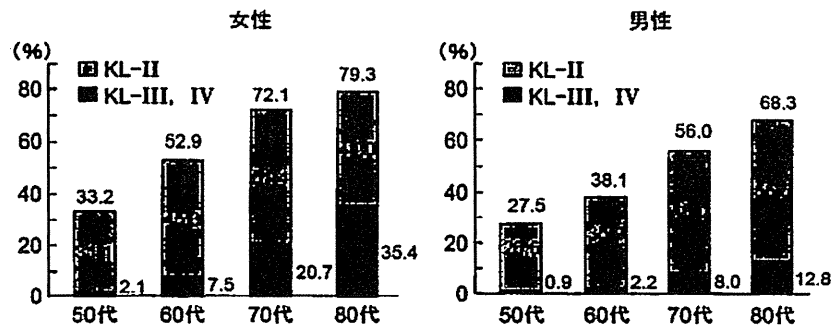

図1　膝関節の変形のある割合

[1)] 国立長寿医療研究センター整形外科，[2)] 愛知淑徳大学健康医療科学部，[3)] 国立長寿医療研究センター予防開発部

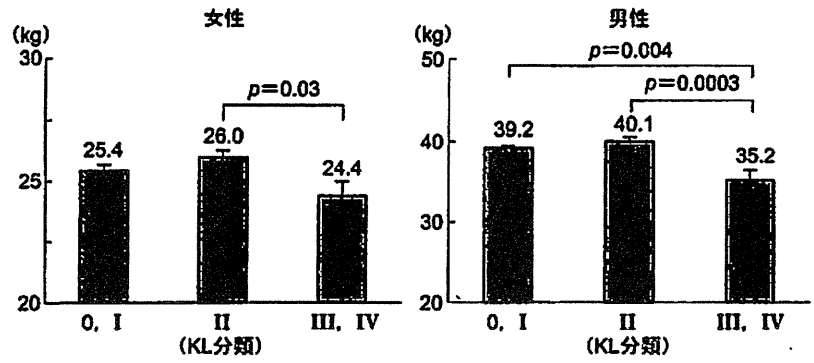

図2　変形の程度による膝伸展筋力の比較
年齢，BMIを調整（平均値±SE）

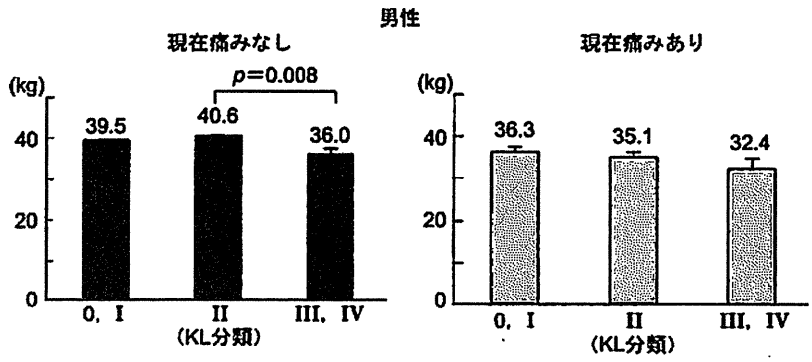

図3　痛みの有無別での変形の程度による膝伸展筋力の比較
年齢，BMIを調整（平均値±SE）

＝0.03）（図2）。また男性においては，正常例39.2±0.29kg，軽度変形例40.1±0.36kg，重度変形例35.2±1.21kgであり，正常と重度変形例，軽度変形と重度変形例の間に有意差を認めた（各 $p=0.004$, $p=0.0003$）（図2）。さらに，現在の痛みの有無別での検討においては，女性では，現在痛みのない群，ある群とも，膝伸展筋力は変形の程度による差を認めなかったが，男性では，現在痛みのない群で，軽度変形と重度変形例の間に有意差を認めた（$p=0.008$）（図3）。

3　考　　察

膝OAの症状改善に大腿四頭筋筋力訓練が有効であることが知られているが，膝関節の変形の程度と同筋力の関連を調べた疫学調査は限られており，一般住民における実態はいまだ不明な点が多い。過去の主な横断的な疫学研究においては，欧米の報告ではSlemandaらはKL分類Ⅱ度以上は，膝伸展筋力（体重比）が関節変形のない群より約20%低下しており，同筋力が10lb-ft増加するごとの膝OAありのオッズ比は0.8であったと報告している[2]。Bakerらは，大腿四頭筋筋力低下は，女性では脛骨大腿関節型膝OA，膝蓋大腿関節型膝OA，両混合型膝OAの有病率と関連し，男性では両混合型膝OAでのみ関連していたとしている[3]。わが国においては，松代膝検診ではKL分類進行に伴い男女ともに大腿四頭筋筋力は低下し，女性はKL分類Ⅱ度とⅢ度の間において，男性はKL分類Ⅲ度とⅣ度の間に有意差を認めたと報告されている[4]。ROAD（Research on Osteoarthritis Against Disability）studyの漁村コホートでは，男性はKL分類Ⅳ度

が0度と比べ，女性はKL分類Ⅲ度とⅣ度が0度と比べ膝伸展筋力が有意に低下しており[5]，また，下肢筋力の高い群はKL分類Ⅲ度以上の有病率が男性13.6%，女性14.5%であったのに対し，筋力の低い群では男性28.4%，女性36.1%と，筋力が低い群で有意に高かったと報告されている[6]。これらわが国の報告は，膝関節軽度屈曲位にて等尺性の膝伸展筋力を測定したものである。しかしながら変形性膝関節症では，通常歩行時より椅子からの立ち上がり動作時などのような，膝をより深く曲げた状態での症状が多く，今回の膝関節90度屈曲位での膝伸展筋力と膝関節変形との関連の検討はさらに意義深いと考えられる。結果として，男女ともに，軽度変形例では筋力低下を認めずに重度変形でのみ筋力低下を認め，今回検討した範囲では軽度屈曲位で測定した結果とおおむね同様であった。また痛みの有無別の検討にて男女で違いがあり，今後その意義などの検討が必要である。

結　　語

地域在住中高年者を対象とした大規模コホートにて，膝関節変形の有無や程度と膝伸展筋力との関連を検討した結果，軽度変形例と比べて重度変形例で男女ともに膝伸展筋力の低下をきたしていた。

文　　献

1) 赤居正美，岩谷力，黒澤尚ほか．運動器疾患に対する運動療法の効果に関する実証研究：無作為化比較試験による変形性膝関節症に対する運動療法の効果．日本整形外科学会雑誌 2006;80(5):316-20.
2) Shimokata H, Ando F, Niino N. A new comprehensive study on aging the National Institute for Longevity Science, Longitudinal Study of Aging (NILS-LSA). J Epidemiology 2000;10:S1-9.
3) Slemenda C, Brandt KD, Heilman DK, et al. Quadriceps weakness and osteoarthritis of the knee. Ann Intern Med 1997;127(2):97-104.
4) Baker KR, Xu L, Zhang Y, et al. Quadriceps weakness and its relationship to tibiofemoral and patellofemoral knee osteoarthritis in Chinese: the Beijing osteoarthritis study. Arthritis Rheum 2004;50(6):1815-21.
5) 渡辺博史，古賀良生，大森豪ほか．膝伸展筋力の加齢変化と変形性膝関節症との関連．運動療法と物理療法 2007;18(4):286-91.
6) 村木重之，阿久根徹，岡敬之ほか．膝伸展筋力の年代による推移および変形性膝関節症との相関．The ROAD study. 第12回日本骨粗鬆症学会 2010.
7) 村木重之．筋力と筋量の経年的変化および運動器疾患との関連．医学のあゆみ 2011;236(5):470-4.

Cell Medicine, Vol. 3, pp. 89–95, 2012
Printed in the USA.

2155-1790/12 $90.00 + .00
DOI: http://dx.doi.org/10.3727/215517912X639405
www.cognizantcommunication.com

Cryopreservation of Induced Pluripotent Stem Cells

Yoshitaka Miyamoto,*†‡ Hirofumi Noguchi,§ Hiroshi Yukawa,* Koichi Oishi,*
Kenji Matsushita,† Hisashi Iwata,¶ and Shuji Hayashi*

*Department of Advanced Medicine in Biotechnology and Robotics,
Nagoya University Graduate School of Medicine, Higashi-ku, Nagoya, Japan
†Department of Oral Disease Research, National Center for Geriatrics and Gerontology, Aichi, Japan
‡Clinical Research Center, National Center for Child Health and Development, Tokyo, Japan
§Department of Gastroenterological Surgery, Transplant and Surgical Oncology,
Okayama University Graduate School of Medicine, Dentistry and Pharmaceutical Sciences, Okayama, Japan
¶Department of Biomedical Sciences, Chubu University College of Life and Health Sciences, Aichi, Japan

Induced pluripotent stem (iPS) cells have attracted attention as a promising cell source for medical treatment that could replace marrow stromal cells (MSCs) and adipose tissue-derived stem cells (ASCs). These pluripotent cells can be induced in vitro and in vivo to differentiate into various tissues and organs. The cells will be useful for regenerative medicine, cell therapy, and drug screening. Vitrification is used, as well as a rapid-freeze method, for colony-forming iPS cells. However, the method requires a high degree of technical skill. We herein report a more convenient method for freezing iPS cells in suspension. We examined the proliferation potency of cryopreserved mouse iPS cells using culture medium, 10% DMSO, 10% glycerol, 5% DMSO, 5% glycerol, 5% DMSO+5% glycerol, cell-freezing medium-DMSO, cell-freezing medium-glycerol, Cell Banker 1, Cell Banker 1+, Cell Banker 2, and Cell Banker 3 as cryopreservation solutions. Among them, Cell Banker 3 showed the highest efficacy in terms of the proliferation of mouse iPS cells. The mouse iPS cells cryopreserved in Cell Banker 3 at –80°C for 12 months maintained a high proliferation rate and an undifferentiated status. The formation of teratomas was also examined. In conclusion, Cell Banker 3 allows for freezing of iPS cells in suspension.

Key words: Induced pluripotent stem (iPS) cells; Pluripotency; Cryopreservation; Slow freezing

INTRODUCTION

Induced pluripotent stem (iPS) cells (14,17,23,24) are pluripotent, thus allowing them to differentiate into various cell types, and these cells have a self-renewal capability similar to that of embryonic stem (ES) cells (20,26). The use of ES cells poses the ethical dilemma of requiring the breakdown of fertilized eggs and also is associated with the potential for immune rejection during cell transplantation. These problems can be solved by using iPS cells. Therefore, iPS cells will be useful for regenerative medicine, cell therapy, and drug screening.

Cryopreservation of cells is an essential technique in basic research on cell biology and in clinical use for cell transplantation. Most cell lines and primary cells are provided as frozen cells. A large number of high-quality cells can be supplied to patients at any time by using this technology. Cryopreservation of sperm, ova, and fertilized eggs is currently performed in clinical practice throughout the world. The iPS cells are an alternative promising cell source of pluripotent cells that can be used in place of marrow stromal cells (MSCs) and adipose tissue-derived stem cells (ASCs). However, the viability of human iPS cells decreases significantly during cryopreservation, as does that of human ES cells. To solve this problem, the vitrification technique used for cryopreservation of fertilized eggs, embryos, and oocytes (5,8,18,19) was examined to freeze ES and iPS cells (7,15,21). Vitrification is an effective cryopreservation technique, but the cells are damaged if there is an increase in osmotic pressure. Therefore, more effective and less cell toxic solutions, as well as more convenient techniques, are strongly desired.

The authors have previously reported a new cryopreservation technique in which ES cells and mouse embryonic fibroblast (MEF) feeder cells were seeded on collagen vitrigel (10). The morphology of these ES cells was good, and the survival rate was high after thawing. In contrast to vitrification, slow freezing in suspension is very convenient

Received January 31, 2011; final acceptance April 1, 2011. Online prepub date: May 8, 2012.
Address correspondence to Hirofumi Noguchi, M.D., Ph.D., Department of Gastroenterological Surgery, Transplant and Surgical Oncology, Okayama University Graduate School of Medicine, Dentistry and Pharmaceutical Sciences, 2-5-1 Shikata-cho, Okayama 700-8558, Japan.
Tel: +81-86-235-7257; Fax: +81-86-221-8775; E-mail: noguchih2006@yahoo.co.jp or noguch-h@cc.okayama-u.ac.jp

to perform and is frequently used for the cryopreservation of various other types of cells. However, when this convenient method is used for ES and iPS cells, it is necessary to examine their condition, because such a freezing process can result in low cell viability or a loss of their pluripotency.

In the present study, the effects of cryopreservation solutions containing dimethyl sulfoxide (DMSO) or glycerol and commercially available cryopreservation solutions were compared for mouse iPS cells. We confirmed that mouse iPS cells could be preserved at –80°C for at least a year and that the cells were maintained in an undifferentiated state.

MATERIALS AND METHODS

Materials

Dulbecco's modified Eagle's medium (DMEM), antibiotics (penicillin, streptomycin), and MEM nonessential amino acids solution (NEAA) were purchased from GIBCO BRL, Life Technologies (Grand Island, NY). Fetal bovine serum (FBS, BIO-WEST) was purchased from Funakoshi Co., Ltd. (Tokyo, Japan). Phosphate-buffered saline (PBS), 2-mercaptoethanol (M6250), glycerol, DMSO (D2650), and formaldehyde were obtained from Sigma-Aldrich (St. Louis, MO). Leukemia inhibitory factor (LIF, Chemicon) was from Dainippon Sumitomo Pharma (Osaka, Japan). Hematoxylin and eosin were purchased from Muto Pure Chemicals (Tokyo, Japan). All chemicals were reagent grade and used as received without further purification.

Mice

Nude mice (BALB/cA Jcl-nu) were purchased from Clea Japan (Osaka, Japan). These mouse studies were approved by the institutional animal care and use committees (IACUC).

Cells

The iPS cell line (iPS-MEF-Ng-20D-17) established by Professor S. Yamanaka at Kyoto University was obtained from the Cell Bank of Riken Bioresource Center (22). MEF feeder cells (Chemicon) were purchased from Dainippon Sumitomo Pharma (Osaka, Japan).

iPS Cell and MEF Feeder Cell Culture

Mouse iPS cells were cultured with mitomycin C-treated feeder cell layers as follows. First, MEF cells were cultured at 37°C with 5% CO_2 in MEF culture medium (DMEM supplemented with 10% heat-inactivated FBS and 1% penicillin–streptomycin) and maintained until the cells reached confluence. The cells were then treated with 50 µl of 100×mitomycin C and incubated at 37°C for at least 2 h. The cells were then cultured on 0.1% gelatin-coated plate for more than 5 h. The iPS cells were maintained at 37°C with 5% CO_2 in ES cell culture medium (DMEM containing 15% FBS, 1×NEAA, 1 mM sodium pyruvate, 2 mM 2-mercaptoethanol, 1% penicillin–streptomycin and 1,000 U/ml LIF) on feeder layers of mitomycin-treated MEF cells. The medium was changed to fresh ES cell culture medium everyday, and the cells were passaged every third day (17,22,25).

Cell Freezing and Thawing Procedures

The basal composition of the cryopreservation medium in this study was the same as that of the ES cell culture medium. Cryoprotectant agents (glycerol and DMSO) were added to the ES cell culture medium at concentrations of 5–10%. The other cryopreservation solutions used were the cell-freezing medium-DMSO, cell-freezing medium-glycerol, Cell Banker 1, Cell Banker 1$^+$, Cell Banker 2, and Cell Banker 3. One milliliter of cell suspension containing 5×10^6 cells was quickly transferred to a 2.0-ml freezing tube and frozen at a cooling rate of 1°C/min. After cooling to –80°C, the cells were stored until use (typically from 1 to 12 months). Frozen tubes were placed in a 37°C water bath to thaw until most ice crystals were melted. The cell suspension was then diluted 1:9 with ES cell culture medium and was centrifuged at 100 *g* for 1 min. The supernatant was removed, and the cells were resuspended in fresh medium. Cell viability was assessed using the trypan blue exclusion test. The final concentration of trypan blue (GIBCO BRL, Grand Island, NY) was 0.2% in the experiments.

Proliferation Assay of iPS Cells

The mitomycin-treated MEF cells (2×10^4 cells) were seeded on 0.1% gelatin-coated 24-well plates (BD Biosciences) with 0.5 ml of MEF culture medium. After culture for 24 h, the cryopreserved iPS and MEF cells (3×10^4 cells) were cultured on mitomycin C-treated feeder cell layers. The cell proliferation was evaluated using a Cell Counting Kit-8 (CCK-8; Dojindo Laboratories, Kumamoto, Japan). The CCK-8 reagent (30 µl) was added to each well (300 µl), and the reaction was allowed to proceed for up to 15 min. The absorbance of the sample at 450 nm was measured against a background control using a microplate reader. The cell proliferation was evaluated after 0–72 h.

Teratoma Formation and Histological Analysis

Mouse iPS cells were suspended at 1×10^7 cells/ml in PBS. Nude mice were anesthetized with diethyl ether. A total of 100 µl of the cell suspension (1×10^6 cells) was injected subcutaneously into the dorsal flank of nude mice. Four weeks after the injection, the tumors were surgically dissected from the mice. The samples were weighed, fixed in PBS containing 4% formaldehyde, and embedded in paraffin. The paraffin sections were stained with hematoxylin and eosin.

RESULTS

Cryopreservation of Mouse iPS Cells and MEF Feeder Cells in Various Solutions

The iPS cells and MEF feeder cells were frozen and preserved at –80°C for 3 months. These cells were cryopreserved in the following solutions: ES cell culture medium, ES cell culture medium containing 10% DMSO, ES cell culture medium +10% glycerol, ES cell culture medium +5% DMSO, ES cell culture medium +5% glycerol, ES cell culture medium +5% DMSO, 5% glycerol, cell-freezing medium-DMSO, cell-freezing medium-glycerol, Cell Banker 1, Cell Banker 1+, Cell Banker 2, and Cell Banker 3. In order to investigate the effects of cryopreservation on cell functions, we determined cell viability immediately after thawing (Fig. 1A) and also examined

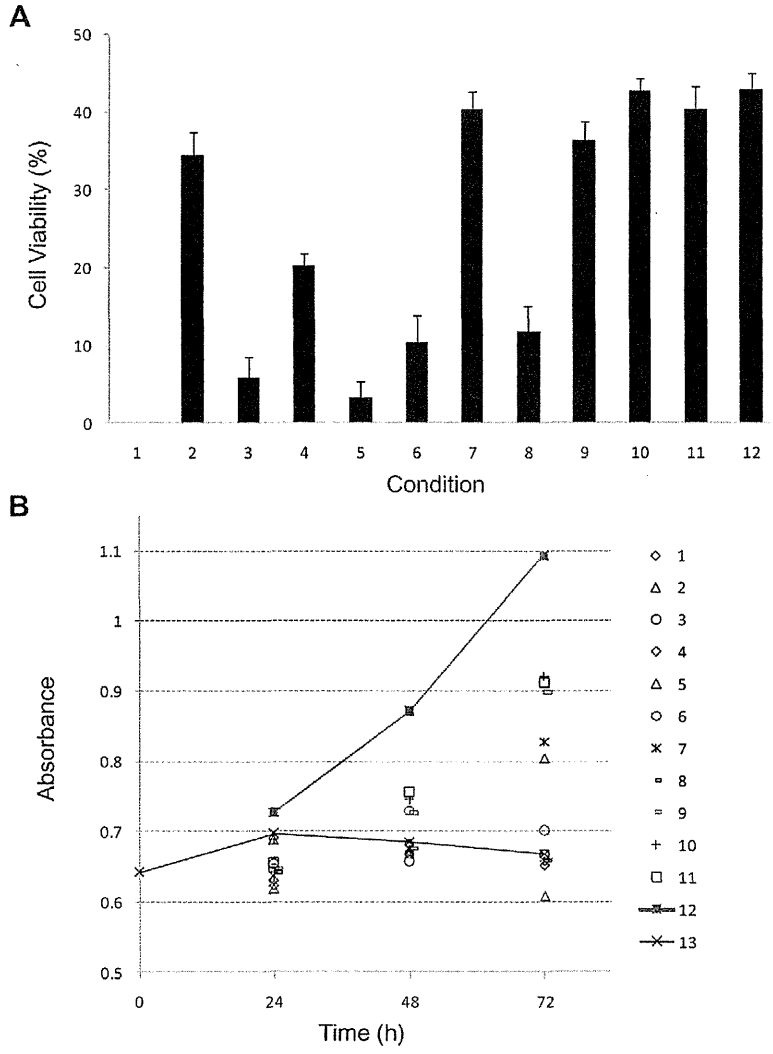

Figure 1. The viability (A) and proliferation (B) of the cryopreserved induced pluripotent stem (iPS) cells frozen using different preservation solutions. 1, Embryonic stem (ES) cell culture medium; 2, ES cell culture medium containing 10% dimethyl sulfoxide (DMSO); 3, ES cell culture medium +10% glycerol; 4, ES cell culture medium + 5% DMSO; 5, ES cell culture medium +5% glycerol; 6, ES cell culture medium +5% DMSO, 5% glycerol; 7, cell-freezing medium-DMSO; 8, cell-freezing medium-glycerol; 9, Cell Banker 1; 10, Cell Banker 1+; 11, Cell Banker 2; 12, Cell Banker 3; 13, only mouse embryonic fibroblast (MEF) feeder cell. The data are the means and SD of three independent experiments.

cell proliferation (Fig. 1B). The viability of iPS cells and MEF feeder cells in 10% DMSO, cell-freezing medium DMSO, Cell Banker 1, Cell Banker 1+, Cell Banker 2, and Cell Banker 3 was shown to be over 30% (Fig. 1A). It was difficult to evaluate the cell viability (10–32%) of only the MEF feeder cells (data not shown). The proliferation of the cells was monitored for 72 h using a commercially available cell-counting reagent (Fig. 1B). The cryopreserved iPS cells in 10% DMSO, cell-freezing medium-DMSO, Cell Banker 1, Cell Banker 1+, Cell Banker 2, and Cell Banker 3 showed higher potency than the MEF feeder cells. The proliferation of the iPS cells frozen in Cell Banker 3 showed the highest proliferation among the 12 cryopreserved solutions. Three days after the inoculation, both iPS and MEF feeder cells adhered and grew well on MEF feeder cell layers (Fig. 2A and B). The cells cryopreserved in 10% DMSO, cell-freezing medium-DMSO, Cell Banker 1, Cell Banker 1+, Cell Banker 2, and Cell Banker 3 were identified as iPS cells. The iPS cells frozen in Cell Banker 1, Cell Banker 1+, Cell Banker 2, and Cell Banker 3 had a morphology similar to that of undifferentiated cells (Fig. 2B; 9–12).

Long-Term Cryopreservation of Mouse iPS Cells and MEF Feeder Cells

To examine the quality of cryopreserved iPS cells in Cell Banker 3 at –80°C for 12 months, we investigated the viability, proliferation, and morphology of the cryopreserved cells (Fig. 3). No significant difference in cell viability or the proliferation rate was observed from the results for iPS cells and MEF feeder cells cryopreserved for 3–12 months (Fig. 3A and B). The cells cryopreserved in Cell Banker 3 were identified as undifferentiated iPS cells (Fig. 3C, 1). Fluorescent microscopy demonstrated that green fluorescent protein genes derived from undifferentiated iPS cells were expressed in these cultures (Fig. 3C, 2).

Teratoma Formation by Cryopreserved Mouse iPS Cells

To evaluate the pluripotency of cryopreserved iPS cells, we transplanted the cells into the dorsal flank of nude mice. The iPS cells produced teratomas after transplantation (Fig. 4A). The teratomas contained various tissues, such as arteries, nerves, cartilage, adipose, and gut epithelium belonging to the three germ layers (endoderm, mesoderm, and ectoderm) (Fig. 4B–F).

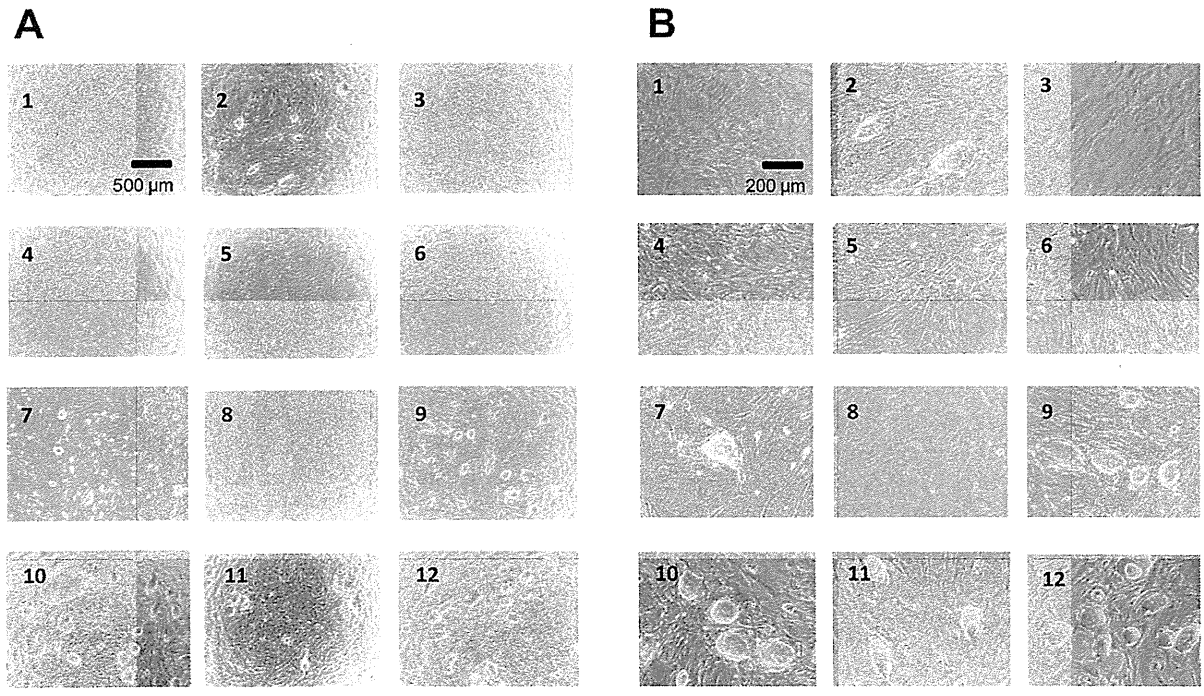

Figure 2. The phase-contrast photomicrographs of iPS cells after cryopreservation (1)–(12). 1, ES cell culture medium; 2, ES cell culture medium containing 10% DMSO; 3, ES cell culture medium + 10% glycerol; 4, ES cell culture medium + 5% DMSO; 5, ES cell culture medium + 5% glycerol; 6, ES cell culture medium +5% DMSO; 5% glycerol; 7, cell-freezing medium-DMSO; 8, cell-freezing medium-glycerol; 9, Cell Banker 1; 10, Cell Banker 1+; 11, Cell Banker 2; 12, Cell Banker 3. The photomicrographs were taken with ×40 (A) and ×100 (B) objectives. The iPS cells were cultured on mitomycin-treated MEF cells for 3 days after inoculation. Scale bars: 500 µm (A) and 200 µm (B).

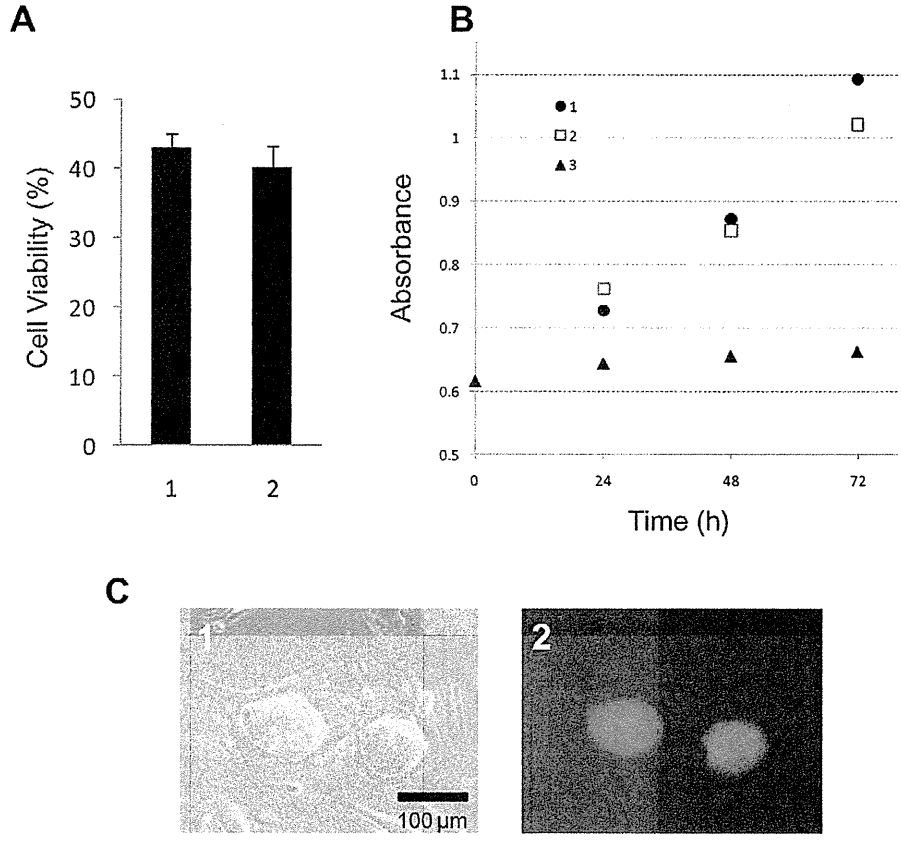

Figure 3. Evaluation of the iPS cells cryopreserved with Cell Banker 3 after 3 and 12 months of storage. (A) The viability of the cryopreserved iPS cells after 3 and 12 months of storage at –80°C. 1, After 3 months; 2, after 12 months. (B) The proliferation of cryopreserved iPS cells after 3 and 12 months of storage. 1, After 3 months; 2, after 12 months; 3, only the MEF feeder cell layer. The data are the means and SD of three independent experiments. (C) The phase-contrast photomicrographs of (1) cryopreserved iPS cells after 12 months. The fluorescent photomicrograph (2) exhibited the expression of green fluorescent protein derived from undifferentiated iPS cells. (C) Scale bar: 100 µm.

DISCUSSION

The iPS cells are a promising cell source for regenerative medicine and cell transplantation therapy. The vitrification process has been used as a rapid-freezing method for colony-forming iPS and ES cells (7,15,21). However, this method requires a high degree of technical skill. We herein report a convenient method for freezing iPS cells in suspension.

In recent years, a wide variety of cryopreservation solutions have been examined to preserve cells without compromising their viability. DMSO and glycerol are conventionally used for the cryopreservation of cells, but they may affect cell functions because of their cytotoxicity (1,9). Either disaccharide trehalose (2–4), oligosaccharide (12), sericin (11,13), or antifreeze proteins (AFP) (6) can be used as a cryopreservation reagent.

In the present study, the functions of cryopreserved iPS cells were investigated using the 12 kinds of newly prepared and commercially available cryopreservation solutions. The iPS cells cryopreserved at –80°C using Cell Banker 3 showed the highest cell viability and proliferation of all the solutions examined in this study (Fig. 1). In addition, the iPS cells cryopreserved in Cell Banker 3 at –80°C for 12 months maintained a high proliferation rate and remained undifferentiated (Fig. 3), and these cells formed teratomas when injected into nude mice (Fig. 4). The cryopreservation technique using Cell Banker 3 can be widely used because it does not require any special technical skills.

The other serum-containing cryopreservation solutions, such as the prepared solutions (DMSO), Cell Banker 1, and Cell Banker 1+, and serum-free Cell Banker 2, were

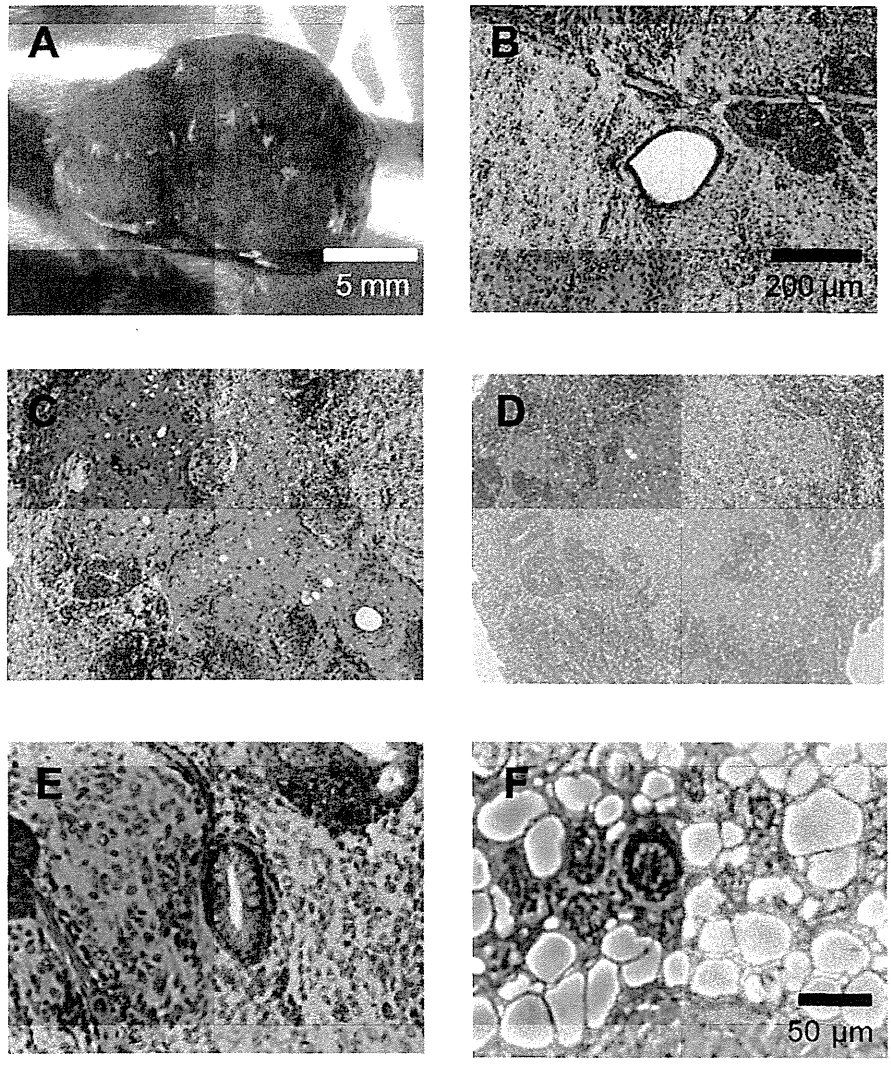

Figure 4. Teratoma formation by iPS cells. Various tissues were present in teratomas derived from iPS cells. (A) Four weeks after the injection, the teratoma was surgically dissected from the mice. (B–F) Slides were stained with hematoxylin and eosin. (B) Artery-like structures. (C) Nerve-like structures. (D) Cartilage-like structures. (E) Gut epithelium-like structures. (F) Adipose-like structures.

also effective for the preservation of iPS cells. In particular, serum-free cryopreservation solutions (Cell Banker 2 and Cell Banker 3) will be useful for regenerative medicine and transplantation.

We previously reported that Cell Banker 2 was effective for the cryopreservation of mouse and human ASCs (11,16). Comparison of the viability, proliferation, and multipotency of mouse ASCs between Cell Banker 2 and Cell Banker 3 showed that Cell Banker 3 led to better preservation of the cells (data not shown). Cell Banker 3 had a similar effect on the preservation of mouse iPS cells as on mouse ASCs and is being used for the preservation of embryos and tissue stem cells, as well as primary hepatocytes, etc.

In conclusion, Cell Banker 3 allows for the effective freezing of iPS cells in suspension.

ACKNOWLEDGMENTS: We thank Ms. Yumie Koshidaka (Nagoya University) for her technical assistance. The present work was supported in part by the Health and Labor Sciences Research Grants from the Ministry of Health, Labour and Welfare. The authors declare no conflicts of interest.

REFERENCES

1. Adler, S.; Pellizzer, C.; Paparella, M.; Hartung, T.; Bremer, S. The effects of solvents on embryonic stem cell differentiation. Toxicol. In Vitro 20:265–271; 2006.
2. Crowe, J. H.; Crowe, L. M. Preservation of mammalian cells—Learning nature's tricks. Nat. Biotechnol. 18:145–146; 2000.
3. Crowe, J. H.; Crowe, L. M.; Jackson, S. A. Preservation of structural and functional activity in lyophilized sarcoplasmic reticulum. Arch. Biochem. Biophys. 220:477–484; 1983.
4. Crowe J. H.; Crowe, L. M.; Mouradian, R. Stabilization of biological membranes at low water activities. Cryobiology 20:346–356; 1983.
5. Dobrinsky, J. R. Advancements in cryopreservation of domestic animal embryos. Theriogenology 57:285–302; 2002.
6. Fletcher, G. L.; Hew, C. L.; Davies, P. L. Antifreeze proteins of teleost fishes. Annu. Rev. Physiol. 63:359–390; 2001.
7. Fujioka, T.; Yasuchika, K.; Nakamura, Y.; Nakatsuji, N.; Suemori, H. A simple and efficient cryopreservation method for primate embryonic stem cells. Int. J. Dev. Biol. 48:1149–1154; 2004.
8. Kuleshova, L.; Gianaroli, L.; Magli, C.; Ferraretti, A.; Trounson, A. Birth following vitrification of a small number of human oocytes: Case report. Hum. Reprod. 14: 3077–3079; 1999.
9. Lovelock, J. E.; Bishop, M. W. Prevention of freezing damage to living cells by dimethyl sulphoxide. Nature 183:1394–1395; 1959.
10. Miyamoto, Y.; Enosawa, S.; Takeuchi, T.; Takezawa, T. Cryopreservation in situ of cell monolayers on collagen vitrigel membrane culture substrata: Ready-to-use preparation of primary hepatocytes and ES cells. Cell Transplant. 18:619–626; 2009.
11. Miyamoto, Y.; Oishi, K.; Yukawa, H.; Noguchi, H.; Sasaki, M.; Iwata, H.; Hayashi, S. Cryopreservation of human adipose tissue-derived stem/progenitor cells using the silk protein sericin. Cell Transplant. 21:617–622; 2012.
12. Miyamoto, Y.; Suzuki, S.; Nomura, K.; Enosawa, S. Improvement of hepatocyte viability after cryopreservation by supplementation of long-chain oligosaccharide in the freezing medium in rats and humans. Cell Transplant. 15:911–919; 2006.
13. Miyamoto, Y.; Teramoto, N.; Hayashi, S.; Enosawa, S. An improvement in the attaching capability of cryopreserved human hepatocytes by a proteinaceous high molecule, Sericin, in the serum-free solution. Cell Transplant. 19:701–706; 2010.
14. Narazaki, G.; Uosaki, H.; Teranishi, M.; Okita, K.; Kim, B.; Matsuoka, S.; Yamanaka, S.; Yamashita, J. K. Directed and systematic differentiation of cardiovascular cells from mouse induced pluripotent stem cells. Circulation 118: 498–506; 2008.
15. Nishigaki, T.; Teramura, Y.; Suemori, H.; Iwata, H. Cryopreservation of primate embryonic stem cells with chemically-defined solution without Me_2SO. Cryobiology 60:159–164; 2010.
16. Oishi, K.; Noguchi, H.; Yukawa, H.; Miyazaki, T.; Kato, R.; Kitagawa, Y.; Ueda, M.; Hayashi, S. Cryopreservation of mouse adipose tissue-derived stem/progenitor cells. Cell Transplant. 17:35–41; 2008.
17. Okita, K.; Ichisaka, T.; Yamanaka, S. Generation of germline-competent induced pluripotent stem cells. Nature 448: 313–317; 2007.
18. Polge, C.; Smith, A. U.; Parkes, A. S. Revival of spermatozoa after vitrification and dehydration at low temperatures. Nature 164:666; 1949.
19. Rall, W. F.; Fahy, G. M. Ice-free cryopreservation of mouse embryos at –196 degrees C by vitrification. Nature 313:573–575; 1985.
20. Reubinoff, B. E.; Pera, M. F.; Fong, C. Y.; Trounson, A.; Bongso, A. Embryonic stem cell lines from human blastocysts: Somatic differentiation in vitro. Nat. Biotechnol. 18:399–404; 2000.
21. Reubinoff, B. E.; Pera, M. F.; Vajta, G.; Trounson, A. O. Effective cryopreservation of human embryonic stem cells by the open pulled straw vitrification method. Hum. Reprod. 16:2187–2194; 2001.
22. Takahashi, K.; Okita, K.; Nakagawa, M.; Yamanaka, S. Induction of pluripotent stem cells from fibroblast cultures. Nat. Protoc. 2:3081–3089; 2007.
23. Takahashi, K.; Tanabe, K.; Ohnuki, M.; Narita, M.; Ichisaka, T.; Tomoda, K.; Yamanaka, S. Induction of pluripotent stem cells from adult human fibroblasts by defined factors. Cell 131:861–872; 2007.
24. Takahashi, K.; Yamanaka, S. Induction of pluripotent stem cells from mouse embryonic and adult fibroblast cultures by defined factors. Cell 126:663–676; 2006.
25. Tateishi, K.; He, J.; Taranova, O.; Liang, G.; D'Alessio, A. C.; Zhang, Y. Generation of insulin-secreting islet-like clusters from human skin fibroblasts. J. Biol. Chem. 283:31601–31607; 2008.
26. Thomson, J. A.; Itskovitz-Eldor, J.; Shapiro, S. S.; Waknitz, M. A.; Swiergiel, J. J.; Marshall, V. S.; Jones, J. M. Embryonic stem cell lines derived from human blastocysts. Science 282:1145–1147; 1998.

Infection and Immunity

E-Selectin Mediates Porphyromonas gingivalis Adherence to Human Endothelial Cells

Toshinori Komatsu, Keiji Nagano, Shinsuke Sugiura, Makoto Hagiwara, Naomi Tanigawa, Yuki Abiko, Fuminobu Yoshimura, Yasushi Furuichi and Kenji Matsushita

Infect. Immun. **2012, 80(7):2570. DOI: 10.1128/IAI.06098-11. Published Ahead of Print 16 April 2012.**

IAI
Journals.ASM.org

E-Selectin Mediates *Porphyromonas gingivalis* Adherence to Human Endothelial Cells

Toshinori Komatsu,[a,b] Keiji Nagano,[c] Shinsuke Sugiura,[a] Makoto Hagiwara,[a] Naomi Tanigawa,[a] Yuki Abiko,[c] Fuminobu Yoshimura,[c] Yasushi Furuichi,[b] and Kenji Matsushita[a,b]

Department of Oral Disease Research, National Center for Geriatrics and Gerontology at Obu, Aichi, Japan[a]; Department of Periodontology and Endodontology, School of Dentistry, Health Sciences University of Hokkaido, Ishikari, Hokkaido, Japan[b]; and Department of Microbiology, School of Dentistry, Aichi-Gakuin University, Nagoya, Aichi, Japan[c]

***Porphyromonas gingivalis*, a major periodontal pathogen, may contribute to atherogenesis and other inflammatory cardiovascular diseases. However, little is known about interactions between *P. gingivalis* and endothelial cells. E-selectin is a membrane protein on endothelial cells that initiates recruitment of leukocytes to inflamed tissue, and it may also play a role in pathogen attachment. In the present study, we examined the role of E-selectin in *P. gingivalis* adherence to endothelial cells. Human umbilical vein endothelial cells (HUVECs) were stimulated with tumor necrosis factor alpha (TNF-α) to induce E-selectin expression. Adherence of *P. gingivalis* to HUVECs was measured by fluorescence microscopy. TNF-α increased adherence of wild-type *P. gingivalis* to HUVECs. Antibodies to E-selectin and sialyl Lewis X suppressed *P. gingivalis* adherence to stimulated HUVECs. *P. gingivalis* mutants lacking OmpA-like proteins Pgm6 and -7 had reduced adherence to stimulated HUVECs, but fimbria-deficient mutants were not affected. E-selectin-mediated *P. gingivalis* adherence activated endothelial exocytosis. These results suggest that the interaction between host E-selectin and pathogen Pgm6/7 mediates *P. gingivalis* adherence to endothelial cells and may trigger vascular inflammation.**

Periodontitis is a disease of the supporting structures of the teeth, causing loss of attachment to the alveolar bone and eventual exfoliation of teeth (5). Severe periodontitis affects up to 20% of the population, and mild to moderate periodontitis is observed in the majority of adults (6). Gram-negative bacteria play an important role in the pathogenesis of human periodontal diseases (15, 42), and *Porphyromonas gingivalis* is one of the species most strongly implicated in periodontal diseases (14, 43). Several recent studies have demonstrated that *P. gingivalis* is able to invade and activate different cell types in the tissue surrounding teeth (endothelial and gingival epithelial cells as well as periodontal ligament cells) (12, 26, 40). Moreover, recent studies have demonstrated a transient bacteremia with potential systemic infection after a variety of dental treatment procedures (2, 19, 20, 41). Therefore, endothelial cells can act as primary target cells during infection with *P. gingivalis*. However, little is known about mechanisms of infection and activation of endothelial cells by *P. gingivalis*.

The endothelium has several important functions, which include providing a nonadhesive, nonthrombotic barrier between the blood and the underlying tissues. In atherosclerosis or in response to injury or inflammatory cytokines such as tumor necrosis factor alpha (TNF-α), the endothelium becomes activated, and selectins and cell adhesion molecules (CAMs) are rapidly induced (36, 39). In particular, members of the immunoglobulin superfamily of CAMs, such as intercellular cell adhesion molecule 1 (ICAM-1) and vascular cell adhesion molecule 1 (VCAM-1), as well as the selectin family members E-selectin and P-selectin, are expressed and play crucial roles in the adhesion and migration of monocyte/macrophage infiltration into atherosclerotic lesions during the early and subsequent stages of atherosclerosis in a variety of animal models (21, 47, 49). Increased expression of E-selectin and production of proinflammatory cytokines in the endothelium play a pivotal role in the generation of leukocyte infiltrates and subsequent atherosclerotic plaque formation (16, 28). *P. gingivalis* infection significantly increases endothelial expression of VCAM-1, ICAM-1, and E-selectin, enhances production of interleukin-6 (IL-6), IL-8, and monocyte chemoattractant protein 1 (MCP-1), and increases adhesion of THP-1 monocytes to endothelial cells (18, 46). Therefore, *P. gingivalis* elicits a proatherogenic response in endothelial cells. Although E-selectin is involved in vascular inflammation and is induced with *P. gingivalis*, the interaction between *P. gingivalis* and endothelial cells is not understood. In the present study, we explored the ability of E-selectin to facilitate *P. gingivalis* adherence to human umbilical vein endothelial cells (HUVECs). We found that activated endothelial cells interact with *P. gingivalis* via E-selectin on endothelial cells and via OmpA-like proteins Pgm6 and -7 of the bacterium.

MATERIALS AND METHODS

Bacterial strains and growth conditions. *P. gingivalis* ATCC 33277 was used as a wild-type strain in this study. *P. gingivalis* defective mutants lacking *fimA* were constructed as described previously (17). A *P. gingivalis* Pgm6/7-deficient mutant was constructed as described previously (32). This mutant did not show any sign of a polar effect on the downstream gene (data not shown). All *P. gingivalis* strains were grown at 37°C under anaerobic conditions (10% CO_2, 10% H_2, and 80% N_2) on brucella HK agar (Kyokuto Pharmaceutical Industrial Co., Ltd., Tokyo, Japan) supple-

Received 27 October 2011 Returned for modification 4 November 2011
Accepted 4 April 2012
Published ahead of print 16 April 2012
Editor: R. P. Morrison
Address correspondence to Kenji Matsushita, kmatsu30@ncgg.go.jp.
Supplemental material for this article may be found at http://iai.asm.org/.

doi:10.1128/IAI.06098-11

mented with 5% laked rabbit blood, hemin (2.5 μg/ml), menadione (5 μg/ml), and dithiothreitol (0.1 mg/ml) and in Trypticase soy broth (BD, Franklin Lakes, NJ) supplemented with yeast extract (2.5 mg/ml), hemin (2.5 μg/ml), menadione (5 μg/ml), and dithiothreitol (0.1 mg/ml). Bacterial growth was monitored by measuring the optical density at 660 nm (OD_{660}). For infection assays, an inoculum with an infection ratio (multiplicity of infection [MOI]) of 100 bacteria per cell was added to the cell culture medium.

Cell culture conditions. HUVECs were cultured in endothelial cell growth medium 2 (EGM-2) (Lonza, Basel, Switzerland) supplemented with fetal bovine serum, hydrocortisone, human recombinant fibroblast growth factor, vascular endothelial growth factor, recombinant insulin growth factor 1, ascorbic acid, human recombinant epidermal growth factor, gentamicin, and amphotericin B at 37°C in a humidified atmosphere of 5% CO_2.

E-selectin expression. E-selectin cDNA was constructed as described previously (53). The E-selectin cDNA was amplified by PCR with specific primers (5′-GAC AGC TAG CAT GAT TGC TTC ACA G-3′ [includes an additional NheI site] and 5′-CGG CCT CGA GTT AAA GGA TGT AAG AAG GC-3′ [includes an additional XhoI site]) and then cloned into the pcDNA3.1 vector (Invitrogen, Carlsbad, CA). For preparation of a soluble E-selectin vector, a stop codon and a unique EcoRV site were introduced by site-directed mutagenesis (Promega, Madison, WI) into the boundary between the sixth consensus repeat and the transmembrane domain, using the following oligonucleotide, which starts at nucleotide 1776: 5′-CC AAC ATT CCC TAG ATA TCT AGA CTT TCT GCT G-3′.

Measurement of E-selectin production. An enzyme-linked immunosorbent assay (ELISA)-based method was used for quantification of E-selectin protein expression in endothelial cells. HUVECs (3.5×10^5 cells/ml) were seeded into 6-well plates and grown overnight. The cells were then stimulated with 10 ng/ml of TNF-α (PeproTec Inc., Rocky Hill, NJ) for 1, 2, 3, 4, 8, and 24 h. After removing the medium, the cell layers were washed twice with phosphate-buffered saline (PBS). Cells were lysed in a cell lysis reagent (CelLytic P; Sigma-Aldrich, St. Louis, MO) with a protease inhibitor mixture (Nacalai Tesque, Kyoto, Japan). Concentrations of E-selectin in the cell lysates were determined using a commercial ELISA kit for E-selectin (eBioscience, San Diego, CA). The cell lysates were also mixed with 4× Laemmli sample buffer without reducing agents and were fractionated by 7.5% SDS-PAGE and immunoblotted with a monoclonal antibody to E-selectin (BBIG-E4 [5D11]; R&D Systems, Abingdon, United Kingdom).

Analysis of *P. gingivalis* adhesion to endothelial cells. HUVECs (2×10^6 cells) were seeded in a Lab-Tek II chamber slide system (Nalge Nunc International, Rochester, NY) that had been coated with 50 μg/ml of rat tail collagen (BD), and the cells were incubated for 24 h before administration of *P. gingivalis*. HUVECs grown to near confluence in each well were stimulated with TNF-α for 3 h, and then *P. gingivalis* cells which had been washed with EGM-2 and resuspended in EGM-2 without antibiotic at a concentration of 10^8 cells/ml were added to the monolayer cells at an MOI of 1:100 under 5% CO_2 at 37°C for 0.5 to 3 h. Cells were then washed three times with PBS, followed each time by gentle rinsing for 5 min at room temperature, and fixed with 4% (wt/vol) paraformaldehyde at 4°C overnight. After washing three times with PBS, the cells were permeabilized with PBS containing 0.05% Triton X-100 at room temperature for 30 min. They were washed again and then blocked with PBS containing 5% (wt/vol) bovine serum albumin (BSA) at room temperature for 30 min. Bacterial cells on chamber slides were labeled with an antiserum for *P. gingivalis* whole cells (1:1,000 dilution) for 60 min at room temperature and then washed five times with PBS. The bacterial cells were then incubated with Alexa Fluor 488-conjugated goat anti-rabbit IgG (1:1,000 dilution; Invitrogen Co., Carlsbad, CA). Actin filaments in HUVECs or 293 cells were stained simultaneously with Alexa Fluor 568-conjugated phalloidin (1 μg/ml; Invitrogen Co.) for 60 min at room temperature in the dark. After washing 10 times with PBS, chamber slides were mounted onto a slide containing ProLong Gold antifade reagent (Invitrogen). Adherent bacteria on the cell surface were examined by fluorescence microscopy (Keyence, Osaka, Japan). We measured the area stained with Alexa 488 (corresponding to *P. gingivalis*) in a visual field (corresponding to 0.06 mm^2) by using the Image J program. We then calculated bacterial number by dividing the area by the size (in pixels) of a *P. gingivalis* cell. To determine whether E-selectin is involved in *P. gingivalis* adherence to endothelial cells, TNF-α-pretreated HUVECs were incubated with *P. gingivalis* ATCC 33277 (10^8 cells/ml in each well) for 30 min to 3 h in the presence of various concentrations of an antibody for E-selectin (R&D Systems, Inc., Minneapolis, MN), recombinant E-selectin, or sialyl Lewis X (Calbiochem, San Diego, CA). *P. gingivalis* ATCC 33277 (10^8 cells/ml in each well) was also incubated with HEK 293 cells transfected with a human E-selectin-inserted vector for 30 min. To explore ligands for E-selectin on *P. gingivalis*, *P. gingivalis* ATCC 33277 (wild type), a FimA-deficient mutant (Δ*fimA*), and a Pgm6/7-deficient mutant (Δ*pgm6/7*) (10^8 cells/ml) were incubated with TNF-α-pretreated HUVECs for 3 h. TNF-α-pretreated HUVECs were incubated with *P. gingivalis* ATCC 33277 (10^8 cells/ml) for 30 min in the presence or absence of envelopes isolated from wild-type or mutant *P. gingivalis*. TNF-α-pretreated HUVECs were incubated with *P. gingivalis* ATCC 33277 (10^8 cells/ml) for 30 min in the presence or absence of purified FimA fimbriae and Pgm6/7.

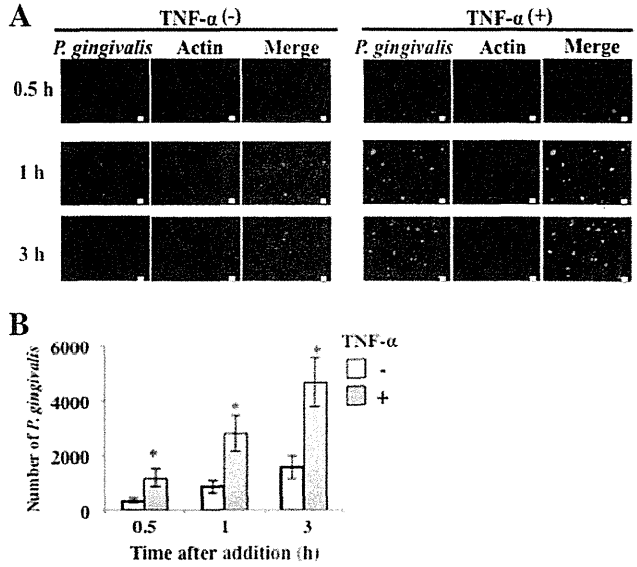

FIG 1 Adherence of *P. gingivalis* to HUVECs is enhanced by stimulation with TNF-α. (A) HUVECs were incubated with TNF-α (10 ng/ml) for 0.5 to 3 h. *P. gingivalis* ATCC 33277 cells (10^8 cells/ml in each well) were then added to the culture medium for 0.5 to 3 h. Cells were then washed, and attachment of *P. gingivalis* to the cells was observed by fluorescence microscopy. *P. gingivalis* was stained with Alexa Fluor 488 (green), and actin of endothelial cells was visualized with Alexa Fluor 568 (red). Bars, 10 μm. (B) HUVECs were incubated with TNF-α (10 ng/ml) for 0.5 to 3 h. *P. gingivalis* ATCC 33277 cells (10^8 cells/ml in each well) were then added to the culture medium for 0.5 to 3 h. Cells were then washed, and attachment of *P. gingivalis* to the cells was observed by fluorescence microscopy. The attachment levels are expressed as numbers of *P. gingivalis* cells per 60,430 mm^2 (means ± standard deviations [SD] [$n = 3$]). *, $P < 0.01$ versus no TNF-α.

Measurement of VWF and nitric oxide. HUVECs (3.5×10^5 cells/ml) were seeded into 12-well plates and grown overnight. The cells were then stimulated with 10 ng/ml of TNF-α for 3 h. *P. gingivalis* cells were inoculated into cultures at an MOI of 100, and the cultures were incubated for 30 min and 1 h. The culture media were then collected and centrifuged at 13,000 rpm for removal of bacterial cells. Concentrations of von Willebrand factor (VWF) in the supernatants were measured by use of an ELISA kit according to the manufacturer's instructions (VWF ELISA kit;

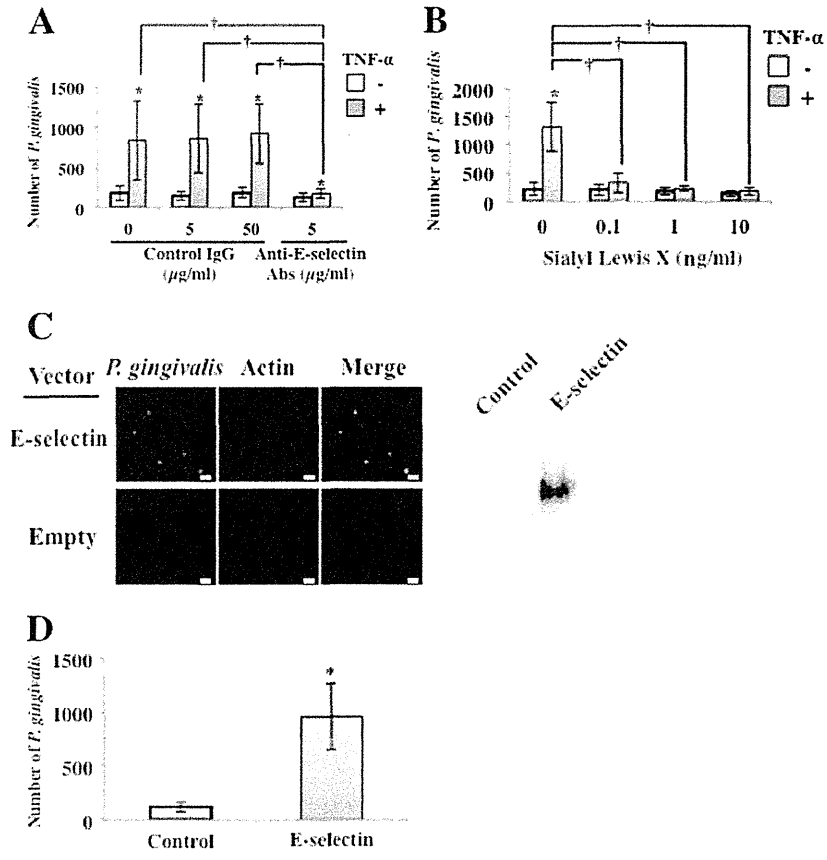

FIG 2 Adherence of *P. gingivalis* to TNF-α-activated endothelial cells was mediated by E-selectin. (A) Inhibitory effect of anti-E-selectin antibodies. HUVECs were incubated with TNF-α (10 ng/ml) for 3 h. Cells were then washed and incubated with *P. gingivalis* ATCC 33277 (10^8 cells/ml in each well) for 30 min in the presence of antibodies for E-selectin or control IgG. Other procedures are described in the legend to Fig. 1B. Data are means ± SD ($n = 3$). *, $P < 0.01$ versus no TNF-α; †, $P < 0.01$ versus no anti-E-selectin antibodies. (B) Inhibitory effect of sialyl Lewis X. HUVECs were incubated with TNF-α (10 ng/ml) for 3 h. Cells were then washed and incubated with *P. gingivalis* ATCC 33277 (10^8 cells/ml in each well) for 30 min in the presence of purified sialyl Lewis X (0 to 10 ng/ml). Other procedures are described in the legend to Fig. 1B. Data are means ± SD ($n = 3$). *, $P < 0.01$ versus no TNF-α; †, $P < 0.01$ versus no sialyl Lewis X. (C) Adherence of *P. gingivalis* was augmented in HEK293 cells transfected with an expression vector for E-selectin. *P. gingivalis* ATCC 33277 (10^8 cells/ml in each well) was incubated with 293 cells transfected with a human E-selectin-inserted vector for 0 min. Other procedures are described in the legend to Fig. 1A. Bars, 10 μm. (D) Adherence of *P. gingivalis* was augmented in 293 cells transfected with an expression vector for E-selectin. *P. gingivalis* ATCC 33277 (10^8 cells/ml in each well) was incubated with 293 cells transfected with a human E-selectin-inserted vector for 30 min. Other procedures are described in the legend to Fig. 1B. Data are means ± SD ($n = 3$). *, $P < 0.01$ versus control.

American Diagnostic Inc., Stanford, CT). The concentration of NO_2^-/NO_3^- was also measured by 2,3-diaminonaphthalene (DAN) assay (24).

Preparation of *P. gingivalis* envelope. Separation of whole envelopes and the outer membrane from *P. gingivalis* strains was performed essentially as described previously (30). Briefly, bacterial cells were washed with PBS (pH 7.5) and then resuspended in PBS (pH 7.5) containing 0.1 mM *N*-α-*p*-tosyl-L-lysine chloromethyl ketone, 0.2 mM phenylmethylsulfonyl fluoride, and 0.1 mM leupeptin. The cells were disrupted by sonication, and remaining, undisrupted bacterial cells were removed by centrifugation at 1,000 × *g* for 10 min. The envelope was collected as a pellet by centrifugation at 100,000 × *g* for 60 min at 4°C. The pellet was washed once by resuspension in PBS and recentrifuged. The final pellet was suspended in PBS.

Purification of FimA. The major fimbriae from *P. gingivalis* ATCC 33277 were purified as described previously (52). The purity was ascertained by scanning of the stained SDS-polyacrylamide gel.

Purification of Pgm6/7 complex. The functional Pgm6/7 complex was purified by two methods. First, we purified it electrophoretically from bacterial envelopes as previously reported (32). Briefly, an envelope fraction of *P. gingivalis* was subjected to SDS-PAGE under nonreducing conditions. A 120-kDa protein band, corresponding to Pgm6/7 heterotrimers, was excised, and then the complex was extracted electrically from a piece of gel. We used these samples for the experiments in Fig. 3E and File S3B in the supplemental material. Second, we constructed C-terminally hexahistidine-tagged Pgm6 and purified the Pgm6/7 complex from a *P. gingivalis* mutant by using a nickel affinity column. Briefly, we inserted a DNA fragment consisting of the *pgm7* open reading frame (ORF) associated with the DNA sequence encoding Gly-Ser-Ser-hexahistidine into the vector pT-COW (13), bearing a powerful promoter of the 350-bp upper region of *ragA* (31). The constructed plasmid was introduced into a *pgm7* deletion mutant of *P. gingivalis* (32). The cell lysate was applied to a nickel affinity column, and the bound proteins were eluted. Although a hexahistidine tag was associated with Pgm7 alone, the Pgm6/7 complex was obtained. We used these samples for the experiments in Fig. 3F and G and File S3C in the supplemental material.

RESULTS

TNF-α augments adherence of *P. gingivalis* to endothelial cells by inducing expression of E-selectin. We first examined induc-

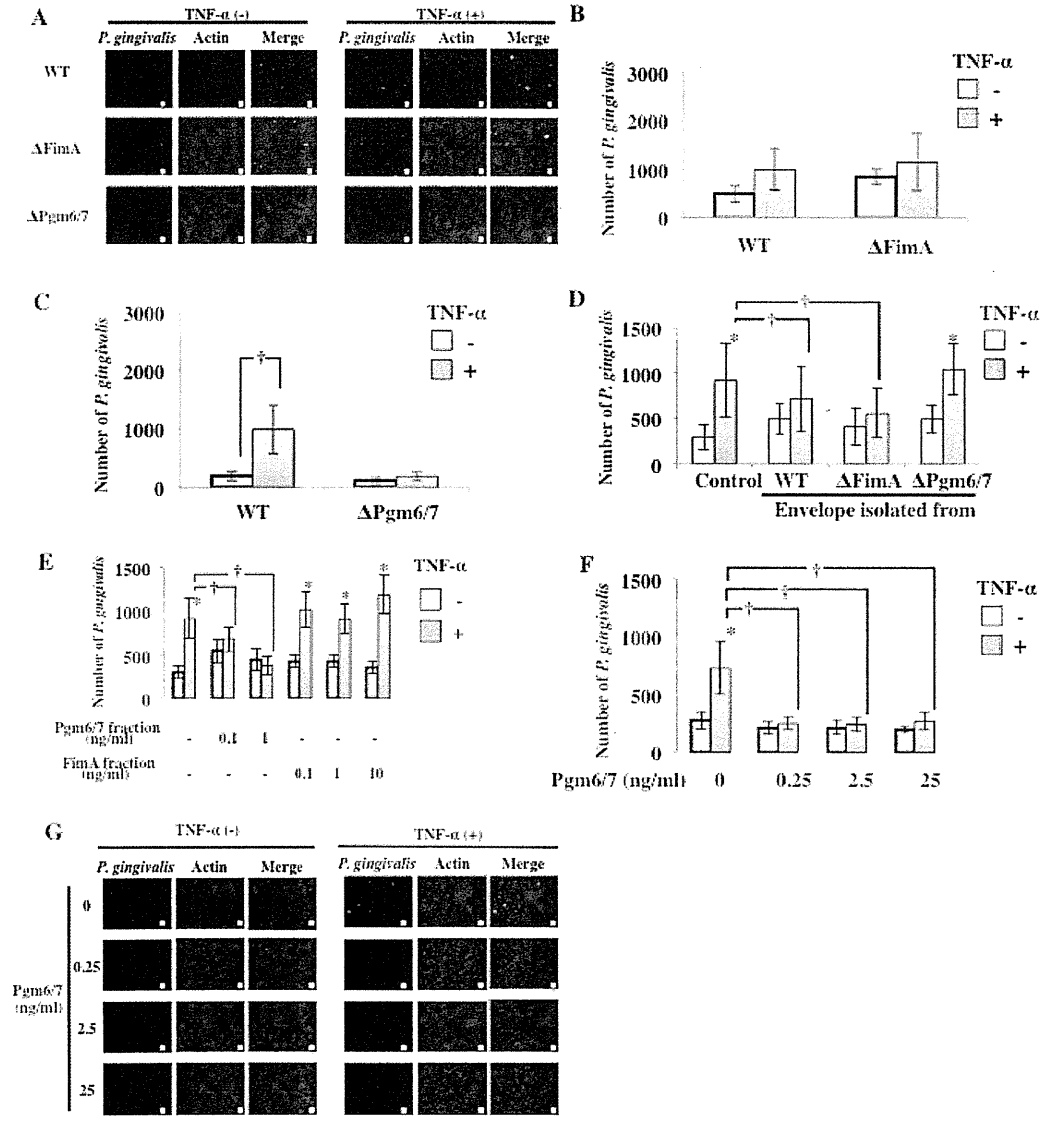

FIG 3 Pgm6/7 in *P. gingivalis* mediates the interaction with activated endothelial cells. (A) *P. gingivalis* ATCC 33277 (wild type), a FimA-deficient mutant (ΔFimA), and a Pgm6/7-deficient mutant (ΔPgm6/7) (10^8 cells/ml in each well) were incubated with TNF-α-pretreated HUVECs for 3 h. Other procedures are described in the legend to Fig. 1A. Bars, 10 μm. (B) *P. gingivalis* ATCC 33277 (wild type) and a FimA-deficient mutant (ΔFimA) (10^8 cells/ml in each well) were incubated with TNF-α-pretreated HUVECs for 30 min. Other procedures are described in the legend to Fig. 1A. (C) *P. gingivalis* ATCC 33277 (wild type) and a Pgm6/7-deficient mutant (Pgm6/7) (10^8 cells/ml in each well) were incubated with TNF-α-pretreated HUVECs for 30 min. Other procedures are described in the legend to Fig. 1B. Data are means ± SD ($n = 3$). *, $P < 0.01$ versus no TNF-α. (D) Inhibitory effects of *P. gingivalis* envelopes on TNF-α-induced adhesion of *P. gingivalis* to HUVECs. HUVECs were incubated with TNF-α (10 ng/ml) for 3 h. Cells were then washed and incubated with *P. gingivalis* ATCC 33277 (10^8 cells/ml in each well) for 30 min in the presence or absence of envelopes isolated from wild-type or mutant *P. gingivalis*. Other procedures are described in the legend to Fig. 1B. Data are means ± SD ($n = 3$). *, $P < 0.01$ versus no TNF-α; †, $P < 0.01$ versus control. (E) Effects of extracted Pgm6/7 and FimA on TNF-α-induced adhesion of *P. gingivalis* to HUVECs. HUVECs were incubated with TNF-α (10 ng/ml) for 3 h. Cells were then washed and incubated with *P. gingivalis* ATCC 33277 (10^8 cells/ml in each well) for 30 min in the presence or absence of purified Pgm6/7 and FimA. Other procedures are described in the legend to Fig. 1B. Data are means ± SD ($n = 3$). *, $P < 0.01$ versus no TNF-α; †, $P < 0.01$ versus Pgm6/7 fraction. (F) Inhibitory effect of *P. gingivalis* Pgm6/7 on TNF-α (10 ng/ml)-induced adhesion of *P. gingivalis* to HUVECs. HUVECs were incubated with TNF-α (10 ng/ml) for 3 h. Cells were then washed and incubated with *P. gingivalis* ATCC 33277 (10^8 cells/ml in each well) for 30 min in the presence or absence of purified Pgm6/7. Other procedures are described in the legend to Fig. 1B. Data are means ± SD ($n = 3$). *, $P < 0.01$ versus no TNF-α; †, $P < 0.01$ versus Pgm6/7 (0 ng/ml). (G) Inhibitory effect of *P. gingivalis* Pgm6/7 on TNF-α-induced adhesion of *P. gingivalis* to HUVECs. HUVECs were incubated with TNF-α (10 ng/ml) for 3 h. Cells were then washed and incubated with *P. gingivalis* ATCC 33277 (10^8 cells/ml in each well) for 30 min in the presence or absence of purified Pgm6/7. Other procedures are described in the legend to Fig. 1A. Bars, 10 μm.

tion of E-selectin expression by TNF-α by using ELISA and Western blotting of HUVEC cultures. TNF-α induced a time-dependent expression of E-selectin in HUVECs (see Files S1 and S2 in the supplemental material). E-selectin expression was maximal 3 h after TNF-α addition. No basal expression of E-selectin was found. To determine whether E-selectin expression in endothelial cells is involved in adhesion of *P. gingivalis* to the cells, we incubated HUVECs with TNF-α (10 ng/ml) for 0.5 to 3 h, and then *P.*

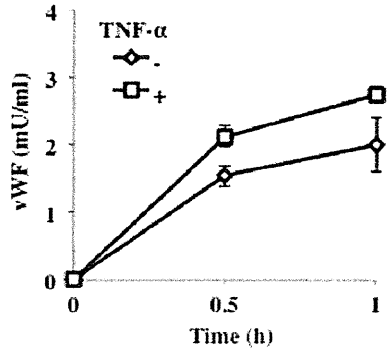

FIG 4 Endothelial VWF exocytosis in response to *P. gingivalis* is augmented by pretreatment with TNF-α. HUVECs were incubated with TNF-α (10 ng/ml) for 3 h. Cells were then washed and incubated with *P. gingivalis* ATCC 33277 (10^8 cells/ml in each well) for 0 to 1 h. The release of VWF into the medium was measured by ELISA. Data are means ± SD ($n = 3$).

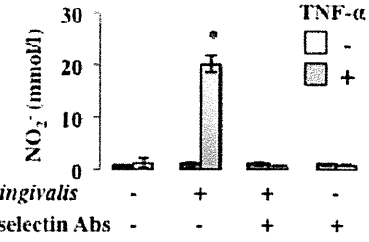

FIG 5 *P. gingivalis*-induced nitric oxide release from activated endothelial cells is mediated by E-selectin. HUVECs were incubated with TNF-α (10 ng/ml) for 3 h. Cells were then washed and incubated with *P. gingivalis* ATCC 33277 (10^8 cells/ml in each well) for 30 min in the presence or absence of an antibody for E-selectin. The release of nitric oxide into the medium was measured by DAN assay. Data are means ± SD ($n = 3$). *, $P < 0.01$ versus no TNF-α.

gingivalis ATCC 33277 cells (10^8 cells/ml in each well) were added to the culture medium for 0.5 to 3 h. Cells were then washed, and attachment of *P. gingivalis* to the cells was observed by fluorescence microscopy. Attachment of *P. gingivalis* to HUVECs increased time dependently without pretreatment of TNF-α (Fig. 1A and B). Pretreatment with 10 ng/ml of TNF-α significantly enhanced the level of attachment in HUVEC cultures.

To clarify the role of E-selectin in *P. gingivalis* adherence to HUVECs, we examined the effect of anti-E-selectin antibodies on *P. gingivalis* adherence to HUVECs. HUVECs were pretreated with TNF-α and then incubated with *P. gingivalis* for 30 min in the presence of antibodies for E-selectin or control IgG. Antibodies to E-selectin inhibited *P. gingivalis* adherence to TNF-α-pretreated HUVECs (Fig. 2A).

E-selectin mediates the rolling of leukocytes on activated endothelial cells through binding of the carbohydrate antigen sialyl Lewis X (37). Therefore, we examined the effect of sialyl Lewis X on interactions between *P. gingivalis* and endothelial cells. Sialyl Lewis X inhibited TNF-α-induced *P. gingivalis* adherence to HUVECs at a concentration of 0.1 μg/ml (Fig. 2B). To assess the effect of E-selectin overexpression on the upregulation of *P. gingivalis* adherence to endothelial cells, we transfected an E-selectin-inserted plasmid into HUVECs. Expression of E-selectin was confirmed by Western blotting 24 h after transfection (Fig. 2C). Adherence of *P. gingivalis* significantly increased in E-selectin-transfected HEK 293 cells (Fig. 2D). These results suggest that TNF-α augments *P. gingivalis* adherence to HUVECs by inducing expression of E-selectin.

***P. gingivalis* interacts with TNF-α-stimulated endothelial cells via Pgm6/7.** The initial adherence of *P. gingivalis* to host cells is mediated by multiple adhesins, including FimA and HagB (44, 45). To determine whether an interaction occurs between the major fimbriae and E-selectin, we examined adherence to endothelial cells of *P. gingivalis* defective in FimA alone (ΔFimA). TNF-α increased the adherence to endothelial cells of FimA-deficient *P. gingivalis* as well as wild-type *P. gingivalis*, and the degrees of adherence were similar (Fig. 3A and B). We next examined whether a major outer membrane protein of *P. gingivalis* that is homologous to the OmpA protein in *Escherichia coli*, namely, the Pgm6/7 complex, mediates *P. gingivalis* adherence to HUVECs. The Pgm6/7-deficient mutant (ΔPgm6/7) was incubated with TNF-α-pretreated HUVECs, and attachment of *P. gingivalis* to the cells was observed. TNF-α increased adherence of wild-type *P. gingivalis* to endothelial cells but failed to increase adherence of ΔPgm6/7 *P. gingivalis* to endothelial cells (Fig. 3C). To clarify whether Pgm6/7 mediates *P. gingivalis* adherence to HUVECs, we prepared envelopes from wild-type, ΔFimA, and ΔPgm6/7 *P. gingivalis* cells and examined the effects on the interaction between wild-type *P. gingivalis* and HUVECs. Envelope peptides from wild-type *P. gingivalis* or ΔFimA *P. gingivalis* suppressed adherence of *P. gingivalis* to TNF-α-pretreated HUVECs (Fig. 3D). However, envelope peptides from ΔPgm6/7 *P. gingivalis* did not affect *P. gingivalis* adherence. In addition, the Pgm6/7 fraction from *P. gingivalis* ATCC 33277 suppressed TNF-α-augmented *P. gingivalis* adherence, but the FimA fraction from the same strain did not (Fig. 3E). Furthermore, purified Pgm6/7 inhibited TNF-α activation of *P. gingivalis* adherence to HUVECs at concentrations as low as 0.25 ng/ml (Fig. 3F and G). These results suggest that the *P. gingivalis* peptide Pgm6/7 plays a role in the adherence of *P. gingivalis* to endothelial cells.

***P. gingivalis* interaction with endothelial cells via E-selectin induces endothelial exocytosis and NO production.** Finally, to determine whether E-selectin-mediated adherence of *P. gingivalis* activates endothelial cells and increases vascular inflammation, we investigated induction of VWF and nitric oxide in TNF-α-pretreated endothelial cells by stimulation with *P. gingivalis*. HUVECs were incubated with TNF-α (10 ng/ml) for 3 h, and then the cells were washed and incubated with *P. gingivalis* for 0 to 1 h. The release of VWF into the medium was measured by ELISA. *P. gingivalis* triggers endothelial exocytosis, as measured by endothelial release of VWF. Release of VWF by stimulation with *P. gingivalis* was also enhanced by pretreatment of HUVECs with TNF-α (Fig. 4). TNF-α pretreatment of HUVECs before *P. gingivalis* stimulation for 30 min significantly increased NO_2^- release into the medium (Fig. 5). Anti-E-selectin antibodies inhibited activation of NO release by *P. gingivalis* in TNF-α-pretreated HUVECs. These results suggest that interaction of *P. gingivalis* with endothelial cells via E-selectin activates the endothelial cells and enhances proinflammatory responses of the cells to this bacterium.

DISCUSSION

P. gingivalis adherence to and invasion of endothelial cells have been reported by several investigators (9, 46). However, this is the first report on the adhesion of activated endothelial cells by *P.*

gingivalis. HUVECs activated by TNF-α increased the adherence of *P. gingivalis* through E-selectin expression, interacting with the OmpA-like proteins Pgm6 and -7 in *P. gingivalis*.

One of the initial events in atherogenesis is the activation of endothelial cells, which then express cell surface adhesion molecules such as endothelial leukocyte adhesion molecule (E-selectin), VCAM-1, and ICAM-1 (8, 10, 22). These endothelial adhesion molecules in turn facilitate the attachment of blood leukocytes to endothelial surfaces (34). In the present study, we demonstrated that one of the periodontopathogens adheres to endothelial cells via E-selectin.

P. gingivalis can invade many cell types, including human oral epithelial cells (33, 51), human gingival fibroblasts or epithelial cells (3, 26), human coronary artery smooth muscle cells, and HCAECs (11). Adhesion of *P. gingivalis* to host cells is multimodal (27) and involves a variety of cell surface and extracellular components, including fimbriae, proteases, hemagglutinins, and lipopolysaccharide (LPS) (8). Among the large array of virulence factors produced by *P. gingivalis*, the major fimbriae (FimA) as well as cysteine proteinases (gingipains) contribute to the attachment to and invasion of many types of mammalian cells, including oral epithelial cells (4) and endothelial cells. *P. gingivalis* strains deficient in FimA fimbriae had an attenuated capacity to adhere to and invade epithelial cells and endothelial cells (33, 46, 51). Invasive *P. gingivalis* strains and their purified fimbriae activate expression of cytokines and cell adhesion molecules in endothelial cells (46). However, our data showed that Pgm6/7 rather than FimA is associated with *P. gingivalis* adherence to TNF-α-treated endothelial cells. Although we do not know exact mechanisms, *P. gingivalis* cells adhere to activated endothelial cells through their Pgm6/7 complex, in a manner different from the fimbria-integrin interaction. TNF-α activates endothelial cells to express adhesion molecules as well as proinflammatory cytokine and chemokine receptors and promotes synthesis and release of a variety of inflammatory cytokines and chemokines to support recruitment of activated leukocytes to an inflammatory lesion (38). TNF-α promotes the inflammatory cascade within the arterial wall during development of atherosclerosis (1). In addition, *P. gingivalis* has been detected within atherosclerotic plaques from vascular tissues (25, 54). Therefore, TNF-α may also augment adherence of *P. gingivalis*, as well as that of leukocytes, in part through inducing E-selectin expression. Weibel-Palade bodies (WPBs) are endothelial granules that store VWF and other vascular modulators (48, 50). Endothelial cells secrete WPBs in response to vascular injury, releasing VWF, which triggers platelet rolling. Endothelial exocytosis is one of the earliest responses to vascular damage and plays a pivotal role in thrombosis and inflammation (29). In this study, we demonstrated that *P. gingivalis* interaction with endothelial cells via E-selectin activates endothelial cells, enhances endothelial exocytosis (Fig. 4), and may enhance atherogenesis and thrombosis (e.g., Buerger disease) (7, 23).

Pgm6/7 in *P. gingivalis*, which shares a low level of homology with *E. coli* OmpA, exists as a heterotrimer comprising Pgm6 and Pgm7 and plays a role in the outer membrane integrity of this organism. OmpA in *E. coli* K1 has been reported to interact with a glycoprotein (Ecgp) of human brain microvascular endothelial cells for invasion (35). Therefore, *P. gingivalis* invasion into endothelial cells should be investigated in the near future, especially regarding whether Pgm6/7 is involved in the invasion. How does Pgm6/7 bind to E-selectin? The adhesion activity of E-selectin is mediated primarily by the binding of sialyl Lewis X on the leukocyte to the carbohydrate-binding domain of the protein. E-selectin recognizes the carbohydrate structure of sialyl Lewis X. Pgm6/7 is also a glycoprotein, and therefore it may bind to E-selectin through its carbohydrate side chain. However, we need additional experiments to reveal the mechanism.

Collectively, in the present study, we clarified a new host-pathogen interaction, i.e., the interaction between Pgm6/7, a major outer membrane protein of *P. gingivalis*, and E-selectin of activated endothelial cells. This finding raises the possibility that chronic infection of the vasculature by pathogens such as *P. gingivalis* could exacerbate systemic vascular diseases such as coronary heart disease, stroke, and diabetes mellitus.

ACKNOWLEDGMENTS

This work was supported by grants-in-aid for scientific research (22390354 and 21659436 to K.M.) from the Ministry of Education, Culture, Sports, Science and Technology, Japan.

REFERENCES

1. Aggarwal BB, Natarajan K. 1996. Tumor necrosis factors: developments during the last decade. Eur. Cytokine Netw. 7:93–124.
2. Amar S, et al. 2003. Periodontal disease is associated with brachial artery endothelial dysfunction and systemic inflammation. Arterioscler. Thromb. Vasc. Biol. 23:1245–1249.
3. Amornchat C, Rassameemasmaung S, Sripairojthikoon W, Swasdison S. 2003. Invasion of Porphyromonas gingivalis into human gingival fibroblasts in vitro. J. Int. Acad. Periodontol. 5:98–105.
4. Andrian E, Grenier D, Rouabhia M. 2006. Porphyromonas gingivalis-epithelial cell interactions in periodontitis. J. Dent. Res. 85:392–403.
5. Brown LJ, Oliver RC, Loe H. 1989. Periodontal diseases in the U.S. in 1981: prevalence, severity, extent, and role in tooth mortality. J. Periodontol. 60:363–370.
6. Burt B. 2005. Position paper: epidemiology of periodontal diseases. J. Periodontol. 76:1406–1419.
7. Chen Z, et al. 2007. Synergistic contribution of CD14 and HLA loci in the susceptibility to Buerger disease. Hum. Genet. 122:367–372.
8. Cutler CW, Kalmar JR, Genco CA. 1995. Pathogenic strategies of the oral anaerobe, Porphyromonas gingivalis. Trends Microbiol. 3:45–51.
9. Deshpande RG, Khan MB, Genco CA. 1998. Invasion of aortic and heart endothelial cells by Porphyromonas gingivalis. Infect. Immun. 66:5337–5343.
10. Dong ZM, et al. 1998. The combined role of P- and E-selectins in atherosclerosis. J. Clin. Invest. 102:145–152.
11. Dorn BR, Dunn WA, Jr, Progulske-Fox A. 1999. Invasion of human coronary artery cells by periodontal pathogens. Infect. Immun. 67:5792–5798.
12. Dorn BR, Dunn WA, Jr, Progulske-Fox A. 2001. Porphyromonas gingivalis traffics to autophagosomes in human coronary artery endothelial cells. Infect. Immun. 69:5698–5708.
13. Gardner RG, Russell JB, Wilson DB, Wang GR, Shoemaker NB. 1996. Use of a modified Bacteroides-Prevotella shuttle vector to transfer a reconstructed beta-1,4-D-endoglucanase gene into Bacteroides uniformis and Prevotella ruminicola B(1)4. Appl. Environ. Microbiol. 62:196–202.
14. Griffen AL, Becker MR, Lyons SR, Moeschberger ML, Leys EJ. 1998. Prevalence of Porphyromonas gingivalis and periodontal health status. J. Clin. Microbiol. 36:3239–3242.
15. Haffajee AD, Socransky SS. 2005. Microbiology of periodontal diseases: introduction. Periodontol. 2000 38:9–12.
16. Hansson GK. 2005. Inflammation, atherosclerosis, and coronary artery disease. N. Engl. J. Med. 352:1685–1695.
17. Hasegawa Y, et al. 2009. Anchoring and length regulation of Porphyromonas gingivalis Mfa1 fimbriae by the downstream gene product Mfa2. Microbiology 155:3333–3347.
18. Hashizume T, Kurita-Ochiai T, Yamamoto M. 2011. Porphyromonas gingivalis stimulates monocyte adhesion to human umbilical vein endothelial cells. FEMS Immunol. Med. Microbiol. 62:57–65.
19. Heimdahl A, et al. 1990. Detection and quantitation by lysis-filtration of

bacteremia after different oral surgical procedures. J. Clin. Microbiol. 28: 2205–2209.
20. Herzberg MC, Weyer MW. 1998. Dental plaque, platelets, and cardiovascular diseases. Ann. Periodontol. 3:151–160.
21. Hope SA, Meredith IT. 2003. Cellular adhesion molecules and cardiovascular disease. I. Their expression and role in atherogenesis. Intern. Med. J. 33:380–386.
22. Iiyama K, et al. 1999. Patterns of vascular cell adhesion molecule-1 and intercellular adhesion molecule-1 expression in rabbit and mouse atherosclerotic lesions and at sites predisposed to lesion formation. Circ. Res. 85:199–207.
23. Iwai T. 2009. Periodontal bacteremia and various vascular diseases. J. Periodontal Res. 44:689–694.
24. Kleinhenz DJ, Fan X, Rubin J, Hart CM. 2003. Detection of endothelial nitric oxide release with the 2,3-diaminonapthalene assay. Free Radic. Biol. Med. 34:856–861.
25. Kurihara N, et al. 2004. Detection and localization of periodontopathic bacteria in abdominal aortic aneurysms. Eur. J. Vasc. Endovasc. Surg. 28:553–558.
26. Lamont RJ, et al. 1995. Porphyromonas gingivalis invasion of gingival epithelial cells. Infect. Immun. 63:3878–3885.
27. Lamont RJ, Jenkinson HF. 1998. Life below the gum line: pathogenic mechanisms of Porphyromonas gingivalis. Microbiol. Mol. Biol. Rev. 62: 1244–1263.
28. Libby P. 2002. Inflammation in atherosclerosis. Nature 420:868–874.
29. Matsushita K, et al. 2003. Nitric oxide regulates exocytosis by S-nitrosylation of N-ethylmaleimide-sensitive factor. Cell 115:139–150.
30. Murakami Y, Imai M, Nakamura H, Yoshimura F. 2002. Separation of the outer membrane and identification of major outer membrane proteins from Porphyromonas gingivalis. Eur. J. Oral Sci. 110:157–162.
31. Nagano K, et al. 2007. Characterization of RagA and RagB in Porphyromonas gingivalis: study using gene-deletion mutants. J. Med. Microbiol. 56:1536–1548.
32. Nagano K, et al. 2005. Trimeric structure of major outer membrane proteins homologous to OmpA in Porphyromonas gingivalis. J. Bacteriol. 187:902–911.
33. Njoroge T, Genco RJ, Sojar HT, Hamada N, Genco CA. 1997. A role for fimbriae in Porphyromonas gingivalis invasion of oral epithelial cells. Infect. Immun. 65:1980–1984.
34. Osterud B, Bjorklid E. 2003. Role of monocytes in atherogenesis. Physiol. Rev. 83:1069–1112.
35. Prasadarao NV, et al. 2003. Cloning and expression of the Escherichia coli K1 outer membrane protein A receptor, a gp96 homologue. Infect. Immun. 71:1680–1688.
36. Read MA, et al. 1995. The proteasome pathway is required for cytokine-induced endothelial-leukocyte adhesion molecule expression. Immunity 2:493–506.
37. Rosen SD, Bertozzi CR. 1994. The selectins and their ligands. Curr. Opin. Cell Biol. 6:663–673.
38. Ross R. 1999. Atherosclerosis—an inflammatory disease. N. Engl. J. Med. 340:115–126.
39. Rothlein R, et al. 1988. Induction of intercellular adhesion molecule 1 on primary and continuous cell lines by pro-inflammatory cytokines. Regulation by pharmacologic agents and neutralizing antibodies. J. Immunol. 141:1665–1669.
40. Sandros J, Papapanou P, Dahlen G. 1993. Porphyromonas gingivalis invades oral epithelial cells in vitro. J. Periodontal Res. 28:219–226.
41. Sconyers JR, Crawford JJ, Moriarty JD. 1973. Relationship of bacteremia to toothbrushing in patients with periodontitis. J. Am. Dent. Assoc. 87: 616–622.
42. Slots J. 1979. Subgingival microflora and periodontal disease. J. Clin. Periodontol. 6:351–382.
43. Slots J, Ting M. 1999. Actinobacillus actinomycetemcomitans and Porphyromonas gingivalis in human periodontal disease: occurrence and treatment. Periodontol. 2000 20:82–121.
44. Sojar HT, Han Y, Hamada N, Sharma A, Genco RJ. 1999. Role of the amino-terminal region of Porphyromonas gingivalis fimbriae in adherence to epithelial cells. Infect. Immun. 67:6173–6176.
45. Song H, Belanger M, Whitlock J, Kozarov E, Progulske-Fox A. 2005. Hemagglutinin B is involved in the adherence of Porphyromonas gingivalis to human coronary artery endothelial cells. Infect. Immun. 73:7267–7273.
46. Takahashi Y, Davey M, Yumoto H, Gibson FC III, Genco CA. 2006. Fimbria-dependent activation of pro-inflammatory molecules in Porphyromonas gingivalis infected human aortic endothelial cells. Cell. Microbiol. 8:738–757.
47. Tedder TF, Steeber DA, Chen A, Engel P. 1995. The selectins: vascular adhesion molecules. FASEB J. 9:866–873.
48. Wagner DD, et al. 1991. Induction of specific storage organelles by von Willebrand factor propolypeptide. Cell 64:403–413.
49. Wang G, et al. 2002. Increased monocyte adhesion to aortic endothelium in rats with hyperhomocysteinemia: role of chemokine and adhesion molecules. Arterioscler. Thromb. Vasc. Biol. 22:1777–1783.
50. Weibel ER, Palade GE. 1964. New cytoplasmic components in arterial endothelia. J. Cell Biol. 23:101–112.
51. Weinberg A, Belton CM, Park Y, Lamont RJ. 1997. Role of fimbriae in Porphyromonas gingivalis invasion of gingival epithelial cells. Infect. Immun. 65:313–316.
52. Yoshimura F, Takahashi K, Nodasaka Y, Suzuki T. 1984. Purification and characterization of a novel type of fimbriae from the oral anaerobe Bacteroides gingivalis. J. Bacteriol. 160:949–957.
53. Yoshizaki K, Wakita H, Takeda K, Takahashi K. 2008. Conditional expression of microRNA against E-selectin inhibits leukocyte-endothelial adhesive interaction under inflammatory condition. Biochem. Biophys. Res. Commun. 371:747–751.
54. Zaremba M, Gorska R, Suwalski P, Kowalski J. 2007. Evaluation of the incidence of periodontitis-associated bacteria in the atherosclerotic plaque of coronary blood vessels. J. Periodontol. 78:322–327.

5. *Porphyromonas gingivalis* ジンジパインによるヒト歯肉上皮細胞における IL-33 発現誘導

多田　浩之[1,2]，島内　英俊[3]，松下　健二[2]

[1]奥羽大学歯学部口腔病態解析制御学講座口腔細菌学分野，[2]独立行政法人国立長寿医療研究センター口腔疾患研究部，[3]東北大学大学院歯学研究科口腔生物学講座歯内歯周治療学分野

はじめに

口腔，肺，皮膚や腸管など粘膜組織において，上皮細胞は細菌，アレルゲンや寄生虫の感染に対して物理的障壁となるのみならず，種々の炎症性サイトカインを生産することで炎症の惹起に係わることが知られている。上皮細胞はさまざまな刺激に応答して interleukin（IL）-33，IL-25 ならびに thymic stromal lymphopoietin（TSLP）などを生産し，これら上皮性サイトカインが肥満細胞や好塩基球を直接刺激することにより Th2 型アレルギー性炎症が誘導される[1]。

歯周炎は細菌感染症であり直接の原因は歯周病関連細菌とデンタルプラークであるが，歯周組織の破壊は主として免疫応答による炎症反応により引き起こされる。歯周炎患者の歯周組織では B 細胞とともに多数の $CD4^+$ T 細胞が検出され，多年にわたり歯周炎の病態における Th1/Th2 バランスについて議論がなされており Th2 細胞が多く検出される報告が優勢であるが，歯周炎の病態形成における Th2 細胞の役割は十分に解明されていない[2]。本稿では，IL-33 の特徴および免疫学役割と歯周炎関連細菌 *Porphyromonas gingivalis* による歯肉上皮細胞からの IL-33 誘導機構についてわれわれの知見を概説したい。

1. IL-33

IL-33 は 2005 年に IL-1 受容体ファミリーに属するコンポーネントである ST2 のリガンドとして発見された[3]。ST2 は Th2 細胞，肥満細胞，好塩基球や好酸球に発現することから，IL-33 は Th2 応答に係わるサイトカインであると考えられた。その点で，IL-33 は IL-17 ファミリーサイトカインである IL-25（IL-17E）と機能が類似している。IL-1 受容体ファミリーの IL-1 や IL-18 はプロドメインを有しており，caspase-1 による蛋白分解を受けて生物活性を有する成熟型に変換される。当初 Schmitz らは，IL-33 と caspase-1 を *in vitro* にて反応させると 30 kDa の前駆体型から 18 kDa の成熟型に変換されることで生理活性が示されると報告したが，その後の実験において caspase-1 による活性型 IL-33 への変換は確認されず，caspase-1 ならびにアポトーシスで活性化される caspase-3 と caspase-7 は IL-33 の C 末端側にある生理活性を有する IL-1 様ドメインを切断し，不活性型 IL-33 へ変換させることが明らかにされた。また，IL-33 は通常のサイトカインの分泌経路を経て生産されるのではなく，感染や傷害により細胞がネクローシスに陥ると生理活性を有する 30 kDa の全長体型 IL-33 が細胞外に放出されることが示された[4]。これらの事実は，IL-33 が HMGB1（high mobility group box 1）や IL-1α のように細胞傷害により細胞外に放出される DAMPs（damage-associated molecular patterns）の機能を有していると考えられる。他方，興味深いことに IL-33 は構成的に核内のヘテロクロマチン領域に局在しており，さまざまな遺伝子の転写制御に係わる可能性が示唆されている[5]。しかしながら，核内 IL-33 がどのように免疫応答および炎症反応に係わるかは不明である。

IL-33 mRNA は組織では脳や脊髄などの中枢神経系，リンパ節，肺，皮膚やパイエル板に発現